JOURNAL OF GUIDANCE, CONTROL, AND DYNAMICS
Vol. 26, No. 6, November–December 2003

Limited Authority Adaptive Flight Control for Reusable Launch Vehicles

Eric N. Johnson* and Anthony J. Calise†
Georgia Institute of Technology, Atlanta, Georgia 30332-0150

In the application of adaptive flight control, significant issues arise due to limitations in the plant inputs, such as actuator displacement limits, actuator rate limits, linear input dynamics, and time delay. A method is introduced that allows an adaptive law to be designed for the system without these input characteristics and then to be applied to the system with these characteristics, without affecting adaptation. This includes allowing correct adaptation while the plant input is saturated and allows the adaptation law to function when not actually in control of the plant. To apply the method, estimates of actuator positions must be found. However, the adaptation law can correct for errors in these estimates. Proof of boundedness of system signals is provided for a single hidden-layer perceptron neural network adaptive law. Simulation results utilizing the methods introduced for neural network adaptive control of a reusable launch vehicle are presented for nominal flight and under failure cases that require considerable adaptation.

Nomenclature

A	=	derivative of tracking error time derivative with respect to tracking error
a	=	sigmoidal activation potential
B	=	derivative of tracking error time derivative with respect to pseudocontrol
$\boldsymbol{e}$	=	tracking error
$\boldsymbol{f}(\cdot)$	=	plant dynamics
$\boldsymbol{g}(\cdot)$	=	actuator dynamics or actuator static map
I	=	identity matrix
K_p, K_d	=	diagonal gain matrices: proportional and derivative on model tracking error
K_r	=	diagonal robustifying term gain matrix
L	=	Lyapunov function
m	=	number of plant inputs, that is, number of actuators
n	=	number of plant degrees of freedom and number of neural network outputs
n_1, n_2	=	number of neural network inputs and number of neural network hidden-layer neurons, respectively
P, Q	=	positive definite matrices, reference model tracking Lyapunov equation
$\boldsymbol{r}$	=	weighted sum of tracking error
W, V, Z	=	neural network input and output weights
$\boldsymbol{x}$	=	plant configuration variables
$\boldsymbol{x}_c$	=	external configuration variable command
$\boldsymbol{x}_{\text{in}}$	=	neural network inputs
$\boldsymbol{x}_{\text{rm}}$	=	reference model configuration variables
$\bar{\boldsymbol{x}}$	=	neural network inputs augmented with a bias
Γ_w, Γ_v	=	diagonal matrices containing neural network learning rates
$\boldsymbol{\Delta}(\cdot)$	=	model error function
$\hat{\boldsymbol{\delta}}$, $\boldsymbol{\delta}$, $\boldsymbol{\delta}_{\text{cmd}}$	=	actuator position estimates, actuator positions, and actuator commands, respectively
ε	=	model error neural network reconstruction error
κ	=	e-modification parameter
$\lambda(\cdot)$	=	eigenvalue
$\boldsymbol{\nu}$	=	total pseudocontrol
$\boldsymbol{\nu}_{\text{ad}}$	=	output of neural network
$\boldsymbol{\nu}_{\text{crm}}$	=	reference model pseudocontrol
$\boldsymbol{\nu}_h$	=	hedge signal
$\boldsymbol{\nu}_{\text{pd}}$	=	proportional–derivative pseudocontrol
$\boldsymbol{\nu}_r$	=	robustifying pseudocontrol signal
$\boldsymbol{\sigma}(\cdot)$, $\sigma'(\cdot)$	=	neuron sigmoidal function, gradient of sigmoidal function

Presented as Paper 2000-4157 at the AIAA Guidance, Navigation, and Control Conference, Denver, CO, 14–17 August 2000; received 13 December 2001; revision received 23 May 2003; accepted for publication 9 June 2003.

*Assistant Professor, School of Aerospace Engineering, 270 Ferst Drive. Member AIAA.

†Professor, School of Aerospace Engineering, 270 Ferst Drive. Fellow AIAA.

I. Introduction

THE application of adaptive flight control to reusable launch vehicles (RLVs), as well as other vehicles, is motivated by the potential for cost and safety improvements. However, this application brings about several design integration issues, including those related to limited control authority and flight certification.

Adaptive Flight Control for Reusable Launch Vehicles

Reducing the cost of placing payloads into Earth orbit has been a driving force in space research for several decades. To achieve the cost benefits of airplanelike operations, the amount of analysis and testing required per mission needs to be reduced over that currently performed. Airplanelike operations imply that payload/fuel parameters (weight and balance) and route selection are the only parameters related to flight control that are required to be updated for any flight. This is a goal for future RLV flight control, where the flight control system is designed and tested to operate within a prescribed envelope of possible choices. It has been estimated that this level of improvement could save three man-years of labor per RLV mission.

Launch vehicle flight control is conventionally carried out by linearizing the system at a series of operating points and gain scheduling. Gain scheduling has a distinct drawback for the RLV: The number of required gains to be scheduled becomes very large. If one also requires that these gains allow for a range of possible missions, payloads, and anticipated failure modes, then this approach can become prohibitive. Several approaches are also being pursued as alternatives to gain tables for RLV application.[1] This includes nontraditional approaches such as sliding mode control, where issues such as actuator saturation are also being addressed.[2,3]

In recent years, several theoretical developments have given rise to the use of artificial neural networks (NNs) that learn online for adaptive control of nonlinear systems. These developments are summarized in Refs. 4 and 5. The use of NN adaptive flight control has been demonstrated in piloted hardware-in-the-loop simulation and

flight test on the X-36 aircraft.[6,7] This approach has also been utilized to enable a single controller to handle multiple versions of guided munitions.[8] The fact that this architecture enables adaptation to a nonlinear and nonaffine-in-control plant in real time makes it an attractive candidate to replace RLV gain tables. This approach has the additional benefit that recovery from a class of vehicle component failures has been demonstrated. This latter property is being exploited in development of fault-tolerant flight control systems for civilian transport aircraft[9] and in design of high-bandwidth controllers for unmanned helicopters[10]; it is expected to have a similar potential for the RLV.[11] These fault-tolerance properties also invite a comparison with other approaches to reconfigurable control.[12]

Design Integration Problems in Adaptive Control

Adaptive control theory usually considers only full authority controllers and avoids issues related to input dynamics, saturation, and other system input characteristics by assumption. This conflicts with the fact that real systems have these characteristics.

Input Saturation and Nonadaptive Controllers

Input saturation is a problem for both adaptive and nonadaptive control.[13] Considerable work has been done for nonadaptive systems in the presence of input saturation, particularly those in which the plant is otherwise linear.[14] An important class of methods for dealing with the influence of saturation on integral action is antiwindup bumpless transfer (AWBT) theory.[15] Beyond windup protection, the control system designer must address the issue of maximizing the domain of attraction of nonadaptive systems subject to input saturation.[16,17] Also, there are nonlinear optimal control results developed that can be utilized to produce control histories that meet input constraints,[18] which is an important way to deal with saturation for nominal responses. However, simply allowing only sufficiently conservative commands can be effective, which is the approach taken for space shuttle attitude control.[19] Other methods inherently design-in the actuator limits in nonlinear feedback laws.[20]

Input Saturation and Adaptive Controllers

Input saturation and input rate saturation present a significant problem for adaptive control, perhaps even more so than for nonadaptive control. Saturation violates any affine in control assumption, which is common in the literature. It also violates the assumption that the sign of the effect of the control is known and nonzero because the effect of additional control input is effectively zero once saturation is encountered. These effects can dramatically reduce the domain of attraction. However, unlike a linear controller designed for a specified linear response, it is theoretically possible for the adaptation function, of certain types of adaptive controllers, to continue to function properly during any input saturation.

One approach used is to avoid saturation altogether by command (or sometimes feedback signal) adjustment. This has been demonstrated in an adaptive control setting.[21] At least one method is able to determine exactly how much the command signal needs to be modified to prevent a specific adaptive controller from exceeding saturation limits, potentially removing conservatism.[22] A second category involves slowing or halting adaptation as saturation is entered. A common ad hoc approach for most adaptive control methods is to simply stop adaptation when any input saturates. In the category of slowing adaptation, there are many results that bound the feedback control by some form of a squashing function, such as in Ref. 23, where the absolute upper bound on plant input is approached only asymptotically. Another approach to the problem of adaptive control with input displacement saturation is augmenting the tracking error signal in a model reference adaptive control setting, with an early result given in Ref. 24 without a stability proof. Several approaches have been developed in this category.[21,25–27]

For adaptive control using NNs trained online, there is very little in the literature that relates to input saturation. Current approaches to input position saturation include reducing adaptation rate, as suggested by the theory, to the point of stopping completely once an input is saturated.

The method introduced in this paper (Sec. II) is most closely related to augmented error signal approaches[21,24–27] in that it also relies on removing input characteristics from the error signal used for adaptation. However, the modification is to the reference model itself (instead of the error signal directly). As a result, it is not limited to displacement saturation, linear plants, or linear reference models and may also be applied to quantized or bang–zero–bang control. A consequence is that the reference model becomes dynamically coupled with the plant and the adaptive law during the saturation intervals. The method is fundamentally different than command adjustment, discussed earlier, in the sense that it does not avoid or even prevent saturation. The method introduced here is also related to AWBT theory for nonadaptive controllers, specifically, the Hanus et al. conditioning technique,[28] which, like this work, includes the concept of a mismatch between the commanded and actual plant input, although in this work the mismatch is computed in terms of pseudocontrol.

Linear Input Dynamics

The NN adaptive flight control architecture utilized here generally requires that input dynamics, that is, actuator dynamics, are known or negligible. Improved robustness to unknown input dynamics utilizing more general adaptive control techniques (dynamic nonlinear damping) has been shown.[29] Linear input dynamics present an important issue in this form of NN adaptive control because, although they may often be considered known dynamics, it is not advisable to attempt to cancel them. In the case of a physical actuator, this will lead to excessive driving of the actuator. When a notch filter is introduced to prevent exciting an aeroelastic mode (for example), the control system designer does not want it to be canceled by the adaptation action of the controller. Unfortunately, to regard these input dynamics as unknown or to include them in a dynamic inversion element would result in attempted cancellation in either case. Ideally, the control system designer would like to prevent the adaptive element from attempting to cancel selected linear input dynamics.

Quantized Control

When the input is highly quantized, or simply bang–zero–bang in the extreme example, adaptive control theory is challenged in many of the same ways it is challenged in the input saturation case. For reentry, RLVs often use a combination of continuous aerodynamic controls and bang–zero–bang reaction control system thrusters.[28] Adaptive control methods are also challenged by discrete control. Affinity and knowledge of the sign of control (as a partial derivative) are both violated as with saturation.

Flight Certification

Flight certification requirements relating to flight control vary between military aircraft, civilian aircraft, and spacecraft. In addition, these requirements are evolving to changes in the technology being applied. However, three important issues for adaptive controllers that relate to the work presented here are as follows:

1) Is it possible for the adaptive controller to cause harm to the vehicle? This is a difficult issue for an adaptive controller because it is inherently difficult to show that the controller will not learn incorrectly under reasonable assumptions. Relaxing the assumptions related in input authority is an important step.

2) Can the adaptive element recover from a failure in adaptation? If, for any reason, the adaptive element has learned incorrectly to an extreme level, the adaptive controller should be able to recover. An extreme level of incorrect learning might be characterized by commanding full control deflections when only small deflections are needed. Correct adaptation during input saturation can enable this kind of recovery.

3) Is there a way to verify the adaptation function (in flight test) without risk to the vehicle? This is an important issue for flight certification of adaptive controllers in a research setting. For NN flight control of the X-36 discussed earlier, the first attempt at in-flight adaptation occurred with the adaptive element in the flight control loop. Correct adaptation during arbitrary assignment of the actuator signal enables this type of test to be performed.

Outline

This work extends NN adaptive control laws[4,5,7–9,29,30] to allow the control law designer to prevent adaptation to selected plant input characteristics. In Sec. II, the method is described. Simulation results utilizing the methods introduced for NN adaptive flight control of the X-33, representative of future RLVs, are presented in Sec. III. These results include nominal flight and failure cases that require considerable adaptation. Conclusions are given in Sec. IV, and a proof for the main theorem is given in the Appendix.

II. Pseudocontrol Hedging

The method introduced here is termed pseudocontrol hedging (PCH). The purpose of the method is to prevent the adaptive element of an adaptive control system from attempting to adapt to selected plant input characteristics. The adaptive law is prevented from "seeing" these system characteristics as reference model tracking error by a specific modification of the reference model dynamics. The case of PCH applied to an adaptive control architecture that includes an approximate dynamic inversion is shown in Fig. 1. Here, a NN corrects for errors in the approximate dynamic inversion. Consider the case in which the plant dynamics are of the form

$$\ddot{\boldsymbol{x}} = \boldsymbol{f}(\boldsymbol{x}, \dot{\boldsymbol{x}}, \boldsymbol{\delta}) \tag{1}$$

where $\boldsymbol{x}, \dot{\boldsymbol{x}} \in \Re^n$ and $\boldsymbol{\delta} \in \Re^m$ with $m \geq n$. Assume that an approximate dynamic inversion and control allocation system has developed to determine actuator commands of the form

$$\boldsymbol{\delta}_{\text{cmd}} = \hat{\boldsymbol{f}}^{-1}(\boldsymbol{x}, \dot{\boldsymbol{x}}, \boldsymbol{\nu}) \tag{2}$$

where ν is the pseudocontrol signal and represents a desired $\ddot{x}$ that is expected to be approximately achieved by $\boldsymbol{\delta}_{\text{cmd}}$. That is, this dynamic inversion element was designed without consideration of the actuator model. Then, $\boldsymbol{\delta}_{\text{cmd}} \neq \boldsymbol{\delta}$ due to the asymptotically stable actuators,

$$\dot{\boldsymbol{\delta}} = \boldsymbol{g}(\boldsymbol{\delta}, \boldsymbol{x}, \dot{\boldsymbol{x}}, \boldsymbol{\delta}_{\text{cmd}}) \tag{3}$$

To get the PCH signal $\boldsymbol{\nu}_h$, an estimated actuator position $\hat{\boldsymbol{\delta}}$ is determined based on a model or a measurement. This estimate is then used to get the difference between commanded pseudocontrol and the achieved pseudocontrol,

$$\begin{aligned}\boldsymbol{\nu}_h &= \hat{\boldsymbol{f}}(\boldsymbol{x}, \dot{\boldsymbol{x}}, \boldsymbol{\delta}_{\text{cmd}}) - \hat{\boldsymbol{f}}(\boldsymbol{x}, \dot{\boldsymbol{x}}, \hat{\boldsymbol{\delta}}) \\ &= \boldsymbol{\nu} - \hat{\boldsymbol{\nu}}\end{aligned} \tag{4}$$

With the addition of PCH, the reference model shown in Fig. 1 has a new input, $\boldsymbol{\nu}_h$. If the reference model without PCH was of the form

$$\ddot{\boldsymbol{x}}_{\text{rm}} = \boldsymbol{\nu}_{\text{crm}}(\boldsymbol{x}_{\text{rm}}, \dot{\boldsymbol{x}}_{\text{rm}}, \boldsymbol{x}_c, \dot{\boldsymbol{x}}_c) \tag{5}$$

where $\{\boldsymbol{x}_c, \dot{\boldsymbol{x}}_c\}$ is an external command signal, then the reference model update with PCH is

$$\ddot{\boldsymbol{x}}_{\text{rm}} = \boldsymbol{\nu}_{\text{crm}}(\boldsymbol{x}_{\text{rm}}, \dot{\boldsymbol{x}}_{\text{rm}}, \boldsymbol{x}_c, \dot{\boldsymbol{x}}_c) - \boldsymbol{\nu}_h \tag{6}$$

This particular choice of reference model modification will remove the actuator characteristic from reference model tracking error ($\boldsymbol{e}$, to be discussed) and from the adaptive law. The instantaneous output of the reference model in the feedforward path (Fig. 1) is not changed by the use of PCH and remains $\boldsymbol{\nu}_{\text{crm}}$.

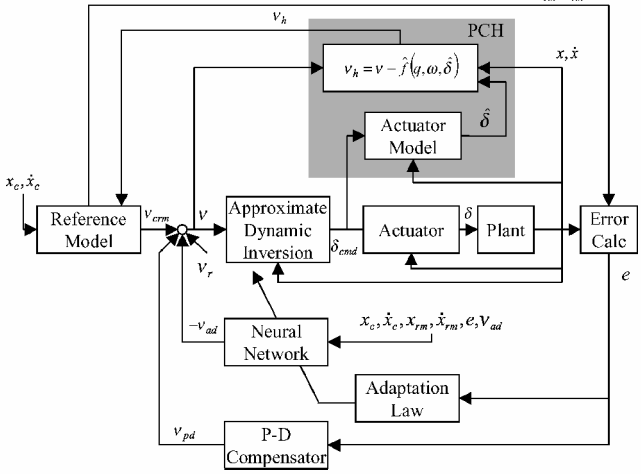

Fig. 1 Model reference adaptive control including an approximate dynamic inversion with PCH compensation.

Reference Model Tracking Error Dynamics

The complete pseudocontrol signal for the system introduced in Fig. 1 with $\boldsymbol{\nu}_{\text{crm}}$ as already described is

$$\boldsymbol{\nu} = \boldsymbol{\nu}_{\text{crm}} + \boldsymbol{\nu}_{\text{pd}} - \boldsymbol{\nu}_{\text{ad}} + \boldsymbol{\nu}_r \tag{7}$$

where $\boldsymbol{\nu}_{\text{ad}}$ and $\boldsymbol{\nu}_r$ are adaptive and robustifying terms to be defined later and $\boldsymbol{\nu}_{\text{pd}}$ is the output of a proportional–derivative compensator acting on reference model tracking error:

$$\boldsymbol{\nu}_{\text{pd}} = K_p(\boldsymbol{x}_{\text{rm}} - \boldsymbol{x}) + K_d(\dot{\boldsymbol{x}}_{\text{rm}} - \dot{\boldsymbol{x}}) \tag{8}$$

When combined into a single vector, reference model tracking error is

$$\boldsymbol{e}^T = \begin{bmatrix}(\boldsymbol{x}_{\text{rm}} - \boldsymbol{x})^T & (\dot{\boldsymbol{x}}_{\text{rm}} - \dot{\boldsymbol{x}})^T\end{bmatrix} \tag{9}$$

The reference model tracking error dynamics are now found by differentiating Eq. (9):

$$\dot{\boldsymbol{e}} = A\boldsymbol{e} + B[\boldsymbol{\nu}_{\text{ad}}(\boldsymbol{x}, \dot{\boldsymbol{x}}, \hat{\boldsymbol{\delta}}) - \boldsymbol{\nu}_r - \boldsymbol{f}(\boldsymbol{x}, \dot{\boldsymbol{x}}, \boldsymbol{\delta}) + \hat{\boldsymbol{f}}(\boldsymbol{x}, \dot{\boldsymbol{x}}, \hat{\boldsymbol{\delta}})] \tag{10}$$

where

$$A = \begin{bmatrix} 0 & I \\ -K_p & -K_d \end{bmatrix}, \qquad B = \begin{bmatrix} 0 \\ I \end{bmatrix} \tag{11}$$

and I the appropriately dimensioned identity matrix.

Remark 1: When one assumes that $\boldsymbol{\delta}$ is exactly known ($\hat{\boldsymbol{\delta}} = \boldsymbol{\delta}$), and v_r is dropped temporarily for clarity, it follows from Eq. (10) that

$$\dot{\boldsymbol{e}} = A\boldsymbol{e} + B[\boldsymbol{\nu}_{\text{ad}}(\boldsymbol{x}, \dot{\boldsymbol{x}}, \boldsymbol{\delta}) - \boldsymbol{\Delta}(\boldsymbol{x}, \dot{\boldsymbol{x}}, \boldsymbol{\delta})] \tag{12}$$

where $\boldsymbol{\Delta}(x, \dot{x}, \delta)$ is model error to be approximately canceled by $\boldsymbol{\nu}_{\text{ad}}$,

$$\boldsymbol{\Delta}(\boldsymbol{x}, \dot{\boldsymbol{x}}, \boldsymbol{\delta}) = \boldsymbol{f}(\boldsymbol{x}, \dot{\boldsymbol{x}}, \boldsymbol{\delta}) - \hat{\boldsymbol{f}}(\boldsymbol{x}, \dot{\boldsymbol{x}}, \boldsymbol{\delta}) \tag{13}$$

and is discussed further later. Equation (12) is of the same form as the model tracking error dynamics seen in previous work[4,5,7–9,29,30] regardless of the actuator. That is, $\boldsymbol{\delta}$ appears rather than $\boldsymbol{\delta}_{\text{cmd}}$.

Remark 2: When one makes the less restrictive assumption that one can express actuator position as a static function of actuator model position and plant state, $\boldsymbol{\delta} = \boldsymbol{\delta}(\boldsymbol{x}, \dot{\boldsymbol{x}}, \hat{\boldsymbol{\delta}})$ (e.g., input saturation occurs earlier than reflected in the model of the actuator), it follows from Eq. (10) that

$$\dot{\boldsymbol{e}} = A\boldsymbol{e} + B[\boldsymbol{\nu}_{\text{ad}}(\boldsymbol{x}, \dot{\boldsymbol{x}}, \hat{\boldsymbol{\delta}}) - \boldsymbol{\Delta}(\boldsymbol{x}, \dot{\boldsymbol{x}}, \hat{\boldsymbol{\delta}})] \tag{14}$$

where

$$\boldsymbol{\Delta}(\boldsymbol{x}, \dot{\boldsymbol{x}}, \hat{\boldsymbol{\delta}}) = \boldsymbol{f}[\boldsymbol{x}, \dot{\boldsymbol{x}}, \boldsymbol{\delta}(\boldsymbol{x}, \dot{\boldsymbol{x}}, \hat{\boldsymbol{\delta}})] - \hat{\boldsymbol{f}}(\boldsymbol{x}, \dot{\boldsymbol{x}}, \hat{\boldsymbol{\delta}}) \tag{15}$$

appears as model error to the adaptive law, which the NN can and does correct for.

Remark 3: When the actuator model contains dynamics and has errors, this will appear as unmodeled input dynamics to the adaptive

law, and alternative methods are appropriate to robustify the adaptive process.[29,30]

Remark 4: It is through selection of the reference model dynamics used in Eq. (6), $\boldsymbol{\nu}_{\text{crm}}$, that the control system designer should address the effects of the actuator on stability and tracking performance. This is done utilizing methods from nonadaptive control, starting with Eqs. (1–3), (6), and (7) and taking

$$\ddot{\boldsymbol{x}}_{\text{rm}} = \boldsymbol{\nu}_{\text{ad}}^* + \hat{\boldsymbol{f}}(\boldsymbol{x}_{\text{rm}}, \dot{\boldsymbol{x}}_{\text{rm}}, \boldsymbol{\delta}) \tag{16}$$

$$\dot{\boldsymbol{\delta}} = \boldsymbol{g}(\boldsymbol{\delta}, \boldsymbol{x}_{\text{rm}}, \dot{\boldsymbol{x}}_{\text{rm}}, \boldsymbol{\delta}_{\text{cmd}}) \tag{17}$$

$$\boldsymbol{\delta}_{\text{cmd}} = \hat{\boldsymbol{f}}^{-1}\left(\boldsymbol{x}_{\text{rm}}, \dot{\boldsymbol{x}}_{\text{rm}}, \boldsymbol{\nu}_{\text{crm}} - \boldsymbol{\nu}_{\text{ad}}^*\right) \tag{18}$$

where $\boldsymbol{\nu}_{\text{ad}}^*$ is an ideal postadaptation output of the adaptive element (precisely defined subsequently) and reference model tracking error is taken as zero. Taken together, these are the zero dynamics of the complete system analyzed herein. When the adaptation method chosen is capable of exactly correcting for model error, Eqs. (16) and (18) become

$$\ddot{\boldsymbol{x}}_{\text{rm}} = \boldsymbol{f}(\boldsymbol{x}_{\text{rm}}, \dot{\boldsymbol{x}}_{\text{rm}}, \boldsymbol{\delta}) \tag{19}$$

$$\boldsymbol{\delta}_{\text{cmd}} = \boldsymbol{f}^{-1}(\boldsymbol{x}_{\text{rm}}, \dot{\boldsymbol{x}}_{\text{rm}}, \boldsymbol{\nu}_{\text{crm}}) \tag{20}$$

respectively, as the nonadaptive design synthesis problem for $\boldsymbol{\nu}_{\text{crm}}$ in simpler form. In the examples given in this paper, the reference model dynamics are chosen as

$$\boldsymbol{\nu}_{\text{crm}} = K_p(\boldsymbol{x}_c - \boldsymbol{x}_{\text{rm}}) + K_d(\dot{\boldsymbol{x}}_c - \dot{\boldsymbol{x}}_{\text{rm}}) \tag{21}$$

where K_p and K_d are fixed gains, which will achieve desirable responses for permissible plant and actuator dynamics. When the actuator is perfect, $\boldsymbol{\delta} = \boldsymbol{\delta}_{\text{cmd}}$, it will correspond to a linear response.

NN as the Adaptive Element

Single hidden-layer perceptron NNs are universal approximators[31] in that they can approximate any smooth nonlinear function to within arbitrary accuracy, given a sufficient number of hidden-layer neurons and input information. Here, a single hidden-layer NN is trained online to cancel model error with feedback, as in Refs. 29, 30, 32, and 33. Figure 2 shows the structure of a single hidden-layer NN. The following definitions are convenient for further analysis.[34] The input–output map can be expressed as

$$\nu_{\text{ad}_k} = b_w\theta_{w,k} + \sum_{j=1}^{n_2} w_{j,k}\sigma_j\left(b_v\theta_{v,j} + \sum_{i=1}^{n_1} v_{i,j}x_{\text{in}_i}\right) \tag{22}$$

where $k = 1, \ldots, 3$. Here n_1, n_2, and n are the number of inputs, hidden-layer neurons, and outputs, respectively, and $x_{\text{in}_i}, i = 1, 2, \ldots, n_1 + 1$ contains the NN inputs. The scalar function σ_j is a sigmoidal activation function, for example,

$$\sigma_j(z) = 1/(1 + e^{-a_j z}) \tag{23}$$

The constant a_j is a distinct value for each hidden-layer neuron, $j = 1, 2, \ldots, n_2$. The maximum of $|a_j|$, for $j = 1, 2, \ldots, n_2$, is $\bar{a}$.

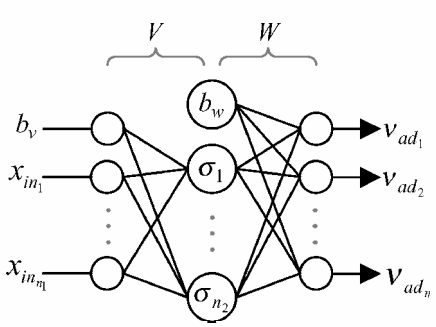

Fig. 2 Single hidden-layer perceptron NN.

For convenience, define the two weight matrices

$$V = \begin{bmatrix} \theta_{v,1} & \cdots & \theta_{v,n_2} \\ v_{1,1} & \cdots & v_{1,n_2} \\ \vdots & \ddots & \vdots \\ v_{n_1,1} & \cdots & v_{n_1,n_2} \end{bmatrix}, \qquad W = \begin{bmatrix} \theta_{w,1} & \cdots & \theta_{w,n} \\ w_{1,1} & \cdots & w_{1,n} \\ \vdots & \ddots & \vdots \\ w_{n_2,1} & \cdots & w_{n_2,n} \end{bmatrix} \tag{24}$$

and define a sigmoid vector as

$$\boldsymbol{\sigma}^T(z) = \begin{bmatrix} b_w & \sigma(z_1) & \sigma(z_2) & \cdots & \sigma\left(z_{n_2}\right) \end{bmatrix} \tag{25}$$

where $b_w > 0$ allows for the threshold θ_w to be included in the weight matrix W,

$$\boldsymbol{z} = V^T\bar{\boldsymbol{x}} \tag{26}$$

$$\bar{\boldsymbol{x}}^T = \begin{bmatrix} b_v & \boldsymbol{x}_{\text{in}}^T \end{bmatrix} \tag{27}$$

where $b_v > 0$ is an input bias that allows for the threshold θ_v to be included in the weight matrix V.

With the preceding definitions, the input–output map of the single hidden-layer NN can be written in a matrix form as

$$\boldsymbol{\nu}_{\text{ad}}(W, V, \bar{\boldsymbol{x}}) = W^T\boldsymbol{\sigma}(V^T\bar{\boldsymbol{x}}) \tag{28}$$

For further convenience, a single matrix containing all tunable NN parameters is defined as

$$Z = \begin{bmatrix} V & 0 \\ 0 & W \end{bmatrix} \tag{29}$$

Also, a matrix containing derivatives of the sigmoid vector is chosen as

$$\boldsymbol{\sigma}'(z) = \begin{bmatrix} 0 & \cdots & 0 \\ \dfrac{\partial\sigma(z_1)}{\partial z_1} & & 0 \\ & \ddots & \\ 0 & & \dfrac{\partial\sigma\left(z_{n_2}\right)}{\partial z_{n_2}} \end{bmatrix} \tag{30}$$

Consider a single hidden-layer perceptron approximation of the nonlinear function $\boldsymbol{\Delta}(\cdot)$, introduced in Eq. (14), over a compact set D of $\bar{\boldsymbol{x}}$. There exists a set of ideal weights $\{W^*, V^*\}$ that brings the output of the NN to within an ε neighborhood of function reconstruction error as long as $\bar{x}$ contains sufficient inputs to reconstruct Δ. This ε neighborhood is bounded by $\bar{\varepsilon}$, defined by

$$\bar{\varepsilon} = \sup_{\bar{x}} \| W^T\boldsymbol{\sigma}(V^T\bar{\boldsymbol{x}}) - \boldsymbol{\Delta}(\bar{\boldsymbol{x}}) \| \tag{31}$$

where the NN inputs x_{in} are chosen to obtain dependency on $\{x, \dot{x}, \hat{\delta}\}$. The universal approximation theorem implies that $\bar{\varepsilon}$ can be made arbitrarily small given a sufficient number of hidden-layer neurons n_2. The matrices W^* and V^* can be defined as the values that minimize $\bar{\varepsilon}$ over D. These values are not necessarily unique. We can also define $\boldsymbol{\nu}_{\text{ad}}^* = W^{*T}\boldsymbol{\sigma}(V^{*T}\bar{\boldsymbol{x}})$ as the corresponding output of the NN.

Finally, define the vector

$$\boldsymbol{r}^T = \boldsymbol{e}^T PB \tag{32}$$

where P is the positive definite solution to the Lyapunov equation $A^T P + PA + Q = 0$. The positive definite choice for Q used here is[35]

$$Q = \begin{bmatrix} K_d K_p & 0 \\ 0 & K_d K_p^2 \end{bmatrix} \frac{1}{\frac{1}{4}n_2 + b_w^2} \tag{33}$$

The robustifying signal is chosen to be

$$\boldsymbol{\nu}_r = -K_r(\|Z\|_F + \bar{Z})(\|\boldsymbol{e}\|/\|\boldsymbol{r}\|)\boldsymbol{r} \tag{34}$$

with $K_r > 0$, $\in \Re^{n\times n}$.

Assumption 1: The true actuator position $\boldsymbol{\delta}$ is related to the estimated value $\hat{\delta}$ by a continuous static map, $\boldsymbol{\delta} = \boldsymbol{\delta}(\boldsymbol{x}, \dot{\boldsymbol{x}}, \hat{\boldsymbol{\delta}})$, corresponding to remark 2.

Assumption 2: The norm of the ideal NN weights is bounded by a known positive value

$$\|Z^*\|_F \le \bar{Z} \tag{35}$$

where $\|\bullet\|_F$ refers to the Frobenius norm

Assumption 3: External commands are bounded:

$$\left\|\begin{bmatrix}\boldsymbol{x}_c^T & \dot{\boldsymbol{x}}_c^T\end{bmatrix}\right\| \le \bar{x}_c \tag{36}$$

Assumption 4: The design process described in remark 4 has resulted in an asymptotically stable nonadaptive subsystem or zero dynamics, and reference model signals remain bounded for permissible plant and actuator dynamics,

$$\left\|\begin{bmatrix}\boldsymbol{x}_{\mathrm{rm}}^T & \dot{\boldsymbol{x}}_{\mathrm{rm}}^T\end{bmatrix}\right\| \le \bar{x}_{\mathrm{rm}} \tag{37}$$

Assumption 5: A fixed point solution exists for the equation $\boldsymbol{\nu}_{\mathrm{ad}} = \boldsymbol{\Delta}$. This assumption is introduced to ensure that the desired condition implied by Eq. (15) is attainable with some error, which under ideal conditions can be made arbitrarily small by a suitably chosen adaptation law. To guarantee existence and uniqueness of a solution, it is sufficient to require that the map $\boldsymbol{\nu}_{\mathrm{ad}} \mapsto \boldsymbol{\Delta}(\boldsymbol{x}, \dot{\boldsymbol{x}}, \boldsymbol{\nu}_{\mathrm{ad}})$ is a contraction, or $\|\partial\boldsymbol{\Delta}/\partial\boldsymbol{\nu}_{\mathrm{ad}}\| < 1$. This is equivalent to the following condition on the approximate plant model $\hat{f}$:

$$\left\|\frac{\partial\boldsymbol{\Delta}}{\partial\boldsymbol{\delta}}\frac{\partial\hat{\boldsymbol{f}}^{-1}}{\partial\boldsymbol{\nu}}\frac{\partial\boldsymbol{\nu}}{\partial\boldsymbol{\nu}_{\mathrm{ad}}}\right\| = \left\|\left(\frac{\partial\boldsymbol{f}}{\partial\boldsymbol{\delta}} - \frac{\partial\hat{\boldsymbol{f}}}{\partial\boldsymbol{\delta}}\right)\frac{\partial\hat{\boldsymbol{f}}^{-1}}{\partial\boldsymbol{\nu}}\right\| = \left\|\frac{\partial\boldsymbol{f}}{\partial\boldsymbol{\delta}}\frac{\partial\hat{\boldsymbol{f}}^{-1}}{\partial\boldsymbol{\nu}} - I\right\| < 1 \tag{38}$$

where for the single input/single output case this condition is satisfied by knowing the sign of control effectiveness (without regard to any actuator limitations), $(\partial\boldsymbol{f}/\partial\boldsymbol{\delta})(\partial\hat{\boldsymbol{f}}/\partial\boldsymbol{\delta}) > 0$, and meeting a lower bound for the estimate of control effectiveness, $|\partial\hat{\boldsymbol{f}}/\partial\boldsymbol{\delta}| > |\partial\boldsymbol{f}/\partial\boldsymbol{\delta}|/2$ (Ref. 36).

Theorem: Consider the system given by Eqs. (1), (3), and the adaptive controller given by Eqs. (2), (4), (6–9), (21), (27), (28), and (32–34) with assumptions 1–5, then the weight adaptation laws

$$\dot{W} = -[(\boldsymbol{\sigma} - \sigma' V^T\bar{\boldsymbol{x}})\boldsymbol{r}^T + \kappa\|\boldsymbol{e}\|W]_w^{\Gamma} \tag{39}$$

$$\dot{V} = -\Gamma_v[\bar{\boldsymbol{x}}\boldsymbol{r}^T W^T\sigma' + \kappa\|\boldsymbol{e}\|V] \tag{40}$$

with restrictions on $\Gamma_w, \Gamma_v, \kappa$, and $\lambda_{\min}(Q)$ [Eq. (A12) in the Appendix], guarantees that reference model tracking error and NN weights are uniformly ultimately bounded.

Proof: See the Appendix.

Corollary: All plant states $\{\boldsymbol{x}, \dot{\boldsymbol{x}}\}$ are uniformly ultimately bounded.

Proof: From uniform ultimate boundedness of reference model tracking error (theorem) and reference model states (assumption 4), uniform ultimate boundedness of plant states is immediate from the definition of reference model tracking error given in Eq. (9).

III. Designs and Results for the X-33

A flight control architecture was tested in MAVERIC,[37] which has been the primary guidance and control simulation tool for the X-33 RLV technology demonstrator program. This work has included flight control design from launch to the beginning of the terminal area energy management phase. Missions include vertical launch and peak Mach numbers of approximately 8 and altitudes of 180,000 ft (55,000 m). During ascent, vehicle mass drops by approximately a factor of three and vehicle inertia by a factor of two. A more exhaustive evaluation of this design is also available.[35]

Ascent Flight Control

The flight control architecture shown in Fig. 1 was utilized for ascent flight control. Nominal inversion consisted of multiplying desired angular acceleration by an estimate of vehicle inertia. A fixed-gain control allocation matrix was selected based on the existing baseline X-33 control allocation system.[38] For ascent, six aerodynamic controls and four aerospike throttles are used. NN inputs were angle of attack, side-slip angle, bank angle, sensed vehicle angular rate, and estimated pseudocontrol $\hat{\boldsymbol{\nu}}$. Four middle-layer neurons were used, learning rates Γ_w on W were unity for all axes, and learning rates Γ_v on V were 20 for all inputs. K_p and K_d were chosen based on a natural frequency of 1.0, 1.5, and 1.5 rad/s^2 for the roll, pitch, and yaw body axes, respectively, and a damping ratio of 0.7. The e-modification parameter κ was chosen to be 0.01. The aerodynamic surface actuator position and rate limits are included in the PCH, as are the position and rate limits of the main engine thrust vectoring. The architecture is shown in Fig. 3.

The resulting flight control system design has no scheduled gains and does not require knowledge of the aerodynamic model of the vehicle. Because aerodynamic moments were neglected when selecting the approximate dynamic inversion, these must be corrected by NN adaptation. This design represents the extreme case of relying on adaptation. Design freedom exists to use scheduled gains or a more accurate approximate dynamic inversion.

Attitude error angles for a nominal ascent phase are shown in Fig. 4. This error is between the guidance command and the vehicle state. Ascent phase ends at main engine cutoff (212 s). Guidance commands are open loop in this case, so that accurate tracking of the command is important. Considerable rate saturation in the aerospike throttles occurs during the initial part of this nominal ascent; therefore, accounting for saturation is essential to the adaptive process even under normal operational conditions.

To illustrate properties of this implementation, a failure case is chosen where it is temporarily not possible to maintain reference model tracking. Near-maximum dynamic pressure, half of the aerodynamic surfaces go hard-over (right rudder full trailing-edge right, right elevons down, right body flap down), resulting in significant model error (Eq. 13). Insufficient control power remains to maintain the command until dynamic pressure drops. The vehicle does three slow rolls to the left before this happens, shown in Fig. 5. The control system had no direct knowledge of these failures; this includes the control allocation, the PCH computation, and the NN. The model error [$\boldsymbol{\Delta}$, Eq. (13)] and NN output [$\boldsymbol{\nu}_{\mathrm{ad}}$, Eq. (28)] for the roll degree

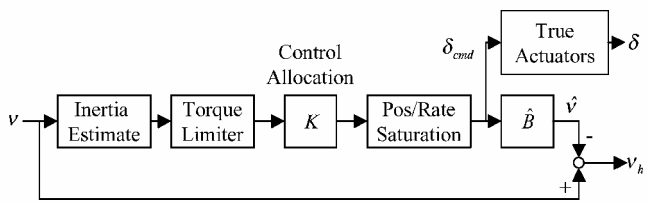

Fig. 3 Determination of pseudocontrol hedge signal, ascent.

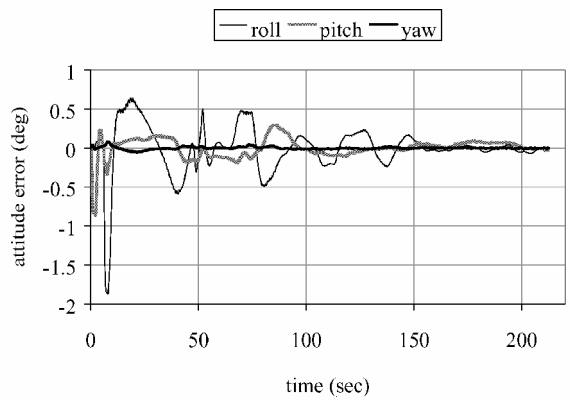

Fig. 4 Attitude error angles for nominal ascent.

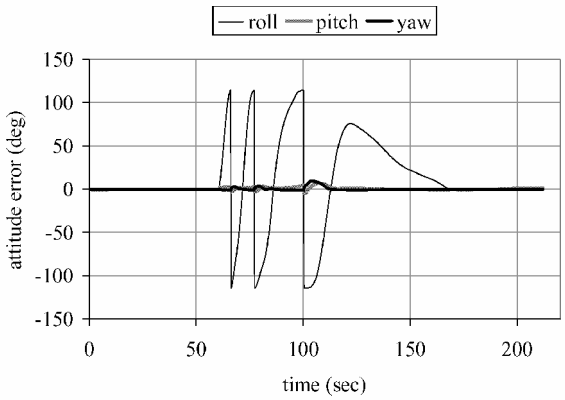

Fig. 5 Multiple actuator hard-overs at 60 s, attitude error angles.

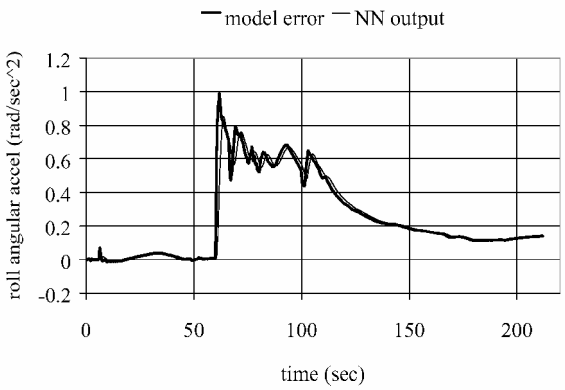

Fig. 6 Multiple actuator hard-overs at 60 s, roll-axis adaptation performance.

of freedom are shown in Fig. 6 and represent roll angular acceleration. During portions of this trajectory, the remaining actuators are at absolute limits; in other portions, they are experiencing axis priority limits. Thus, even though the equilibrium is null controllable, proper tracking is not maintained, and many of the actuators are saturated, adaptation is correct. This correct adaptation enables a rapid recovery once control authority is regained, as shown in Fig. 5. Without PCH both the adaptive controller and the nominal-gain scheduled controller result in an unrecoverable departure.

Entry Flight Control

At the beginning of the entry phase, all NN parameters, inputs, and weight matrices are maintained from the ascent phase. However, a slower linear response was specified to correspond to a reduction in available control power. K_p and K_d were chosen based on a natural frequency of 0.5, 0.8, and 0.7 rad/s^2 for stability-axis roll, pitch, and stability-axis yaw axes, respectively, and a damping ratio of 0.7 for pitch and yaw, and 1.0 for roll. The e-modification parameter κ was chosen to be 0.01 as earlier.

The formulation of the guidance command differs, being an angle-of-attack and angle-of-bank command, rather than an attitude command. This was converted into an attitude command by finding the attitude that corresponds to the specified guidance command, assuming vehicle velocity with respect to the air mass was fixed, that is, regarded as a slow state. Nominal inversion consisted of multiplying desired angular acceleration by an estimate of vehicle inertia and utilizing a fixed-gain control allocation system. Reaction control system jet selection was done by selecting a jet firing combination that corresponded closest to the moment deficit due to aerodynamic actuator limits, with an added penalty on fuel usage. The aerodynamic surface actuator displacement and rate limits were included in the PCH signal, as was reaction control system quantization. The resulting flight control system has no scheduled gains or trim settings and represents an adaptive bang–zero–bang control solution with respect to the reaction control system.

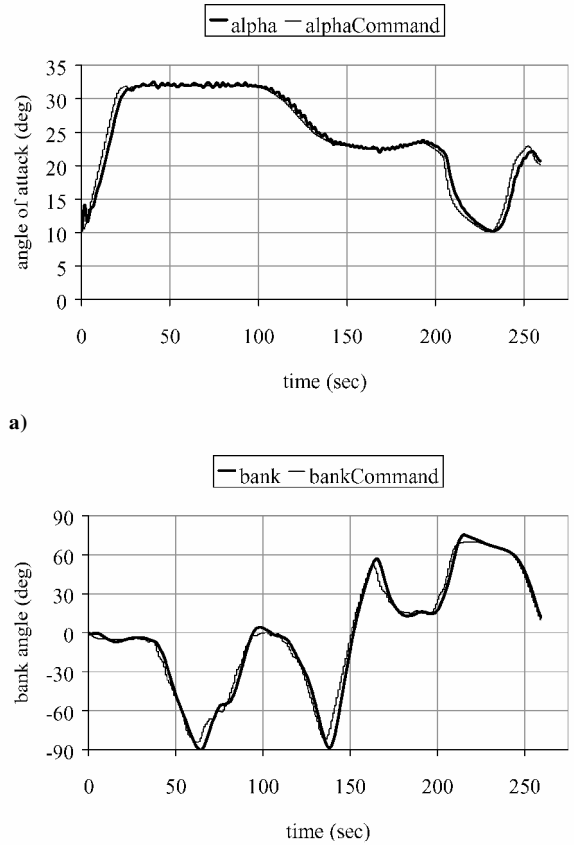

Fig. 7 Command and actual a) angle of attack and b) bank angle for nominal entry.

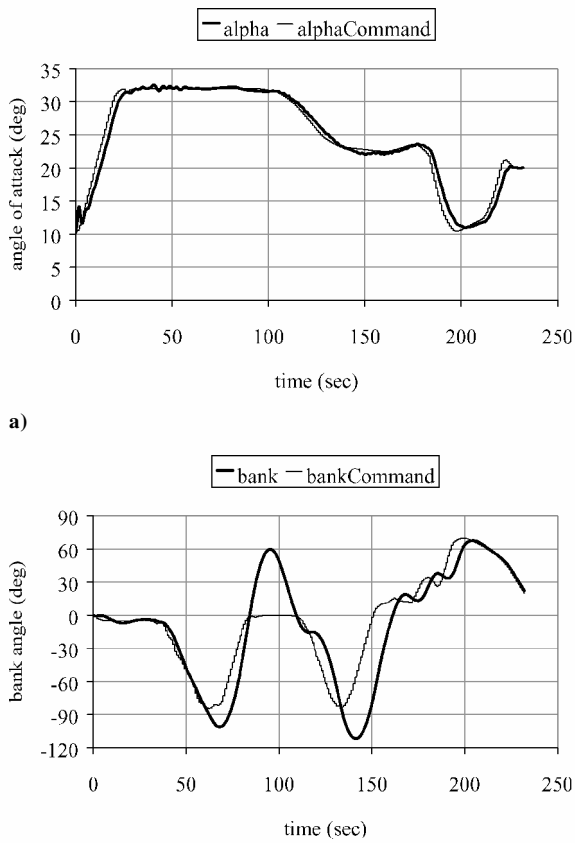

Fig. 8 Command and actual a) angle of attack and b) bank for complete reaction control system failure at 60 s.

Angle of attack and bank angle for nominal transition and entry are shown in Fig. 7. Performance is satisfactory without gain scheduling in the presence of occasional rate saturation of aerodynamic effectors.

Angle of attack and bank angle are shown in Fig. 8 for a complete reaction control system failure occurring 60 s after the beginning of the entry phase. That is, no thrusters are operational after the failure. The flight control system was given no direct knowledge of the failure and so appears as model error. The reduction in available control power has the greatest impact on bank because it has the lowest axis priority in aerodynamic effector control allocation. Although the system is stable, a more conservative guidance command is needed due to the loss of control authority.

IV. Conclusions

The theoretical results presented here are critical in enabling an adaptive flight control system to be used for RLV flight control, where control authority limitations, including the quantized nature of reaction control system control, are routinely encountered even in the absence of failures. The design that was developed and tested achieved desired performance without scheduled gains, trim settings, or knowledge of vehicle aerodynamics, suggesting that little effort would be required to transition to a different vehicle or mission. Adaptation to failure cases was rapid, was effective, and did not require direct knowledge of the failure. Prospects for flight certification of this form of adaptive flight control in general are also improved. Because adaptation is correct during input saturation, the control system is able to recover even if it is temporarily tricked. Also, the adaptive law can be exercised in flight test while not in actual control of the vehicle.

Appendix: Proof of Theorem

Equation (10) can be expressed as

$$\dot{\boldsymbol{e}} = A\boldsymbol{e} + B[\boldsymbol{\nu}_{\text{ad}} + \boldsymbol{\nu}_r - \boldsymbol{\Delta}] \tag{A1}$$

Define $\varepsilon = \boldsymbol{\nu}_{\text{ad}}^* - \boldsymbol{\Delta}$, where $\boldsymbol{\nu}_{\text{ad}}^*$ is the network output using the ideal weights, then Eq. (A1) can be expressed as

$$\dot{\boldsymbol{e}} = A\boldsymbol{e} + B[W^T\boldsymbol{\sigma}(V^T\bar{\boldsymbol{x}}) - W^{*T}\boldsymbol{\sigma}(V^{*T}\bar{\boldsymbol{x}}) + \varepsilon + \boldsymbol{\nu}_r] \tag{A2}$$

where ε is the instantaneous residual network approximation error corresponding to the ideal weights. The difference between the actual and ideal weights is given by $\tilde{W} = W - W^*$ and $\tilde{V} = V - V^*$. When elements of a Taylor series expansion of the sigmoids with respect to W and V are added and subtracted, Eq. (A2) can be rewritten as

$$\dot{\boldsymbol{e}} = A\boldsymbol{e} + B\Big\{\tilde{W}^T[\boldsymbol{\sigma}(V^T\bar{\boldsymbol{x}}) - \sigma'(V^T\bar{\boldsymbol{x}})V^T\bar{\boldsymbol{x}}] + W^T\sigma'(V^T\bar{\boldsymbol{x}})\tilde{V}^T\bar{\boldsymbol{x}} + \boldsymbol{w} + \boldsymbol{\nu}_r\Big\} \tag{A3}$$

where

$$\boldsymbol{w} = \varepsilon - W^{*T}[\sigma(V^{*T}\bar{\boldsymbol{x}}) - \boldsymbol{\sigma}(V^T\bar{\boldsymbol{x}}) + \sigma'(V^T\bar{\boldsymbol{x}})\tilde{V}^T\bar{\boldsymbol{x}}] + \tilde{W}^T\sigma'(V^T\bar{\boldsymbol{x}})V^{*T}\bar{\boldsymbol{x}} \tag{A4}$$

When maximum and minimum values of the sigmoid functions are considered, an upper bound on the norm of $\boldsymbol{w}$ can be written as[7]

$$\|\boldsymbol{w}\| \le c_0 + c_1\|\tilde{Z}\|_F + c_2\|\boldsymbol{e}\|\|\tilde{Z}\|_F + c_3\|\tilde{Z}\|_F^2 \tag{A5}$$

where c_0, c_1, c_2, and c_3, are known constants and the definition of $\tilde{Z}$ follows from the definition given in Eq. (29).

A Lyapunov function candidate is

$$L(\boldsymbol{e}, \tilde{W}, \tilde{V}) = \tfrac{1}{2}\big[\boldsymbol{e}^T P\boldsymbol{e} + \text{tr}\big(\tilde{W}\Gamma_w^{-1}\tilde{W}^T\big) + \text{tr}\big(\tilde{V}^T\Gamma_v^{-1}\tilde{V}\big)\big] \tag{A6}$$

When the weight adaptation laws in Eqs. (39) and (40) are used, the time derivative of L along trajectories can be expressed as

$$\dot{L} = -\tfrac{1}{2}\boldsymbol{e}^T Q\boldsymbol{e} + \boldsymbol{r}^T(\boldsymbol{w} + \boldsymbol{\nu}_r) - \kappa\|\boldsymbol{e}\|\text{tr}(\tilde{Z}^T Z) \tag{A7}$$

which by $-\text{tr}(\tilde{Z}^T Z) = \text{tr}(\tilde{Z}^T Z^*) - \text{tr}(\tilde{Z}^T\tilde{Z}) \le \|\tilde{Z}\|_F\|Z^*\|_F - \|\tilde{Z}\|_F^2$ (Ref. 34) and including the definition of $\boldsymbol{\nu}_r$ in Eq. (34), results in the inequality

$$\dot{L} \le -\tfrac{1}{2}\boldsymbol{e}^T Q\boldsymbol{e} + \|\boldsymbol{r}\|\|\boldsymbol{w}\| - \boldsymbol{r}^T K_r\boldsymbol{r}(\|\boldsymbol{e}\|/\|\boldsymbol{r}\|)(\|Z\|_F + \bar{Z}) - \kappa\|\boldsymbol{e}\|\|\tilde{Z}\|_F^2 + \kappa\|\boldsymbol{e}\|\|\tilde{Z}\|_F\bar{Z} \tag{A8}$$

When the bound on $\boldsymbol{w}$ is used and it is required that

$$\lambda_{\min}(K_r) \ge c_2, \qquad \kappa > \|PB\|c_3 \tag{A9}$$

$\dot{L}$ can be further bounded as

$$\dot{L} \le -\tfrac{1}{2}\lambda_{\min}(Q)\|e\|^2 - (\kappa - \|PB\|c_3)\|\boldsymbol{e}\|\|\tilde{Z}\|_F^2 + a_0\|\boldsymbol{e}\| + a_1\|\boldsymbol{e}\|\|\tilde{Z}\|_F \tag{A10}$$

where

$$a_0 = (\bar{\varepsilon} + 2\bar{Z}(b_w + n_2))\|PB\|$$

$$a_1 = 2\bar{Z}\bar{a}(b_w + n_2)(1 + b_w + n_2)(b_v + \bar{x}_c + \bar{x}_{\text{rm}} + \bar{Z})\|PB\| + \kappa\bar{Z} \tag{A11}$$

By selection of $\lambda_{\min}(Q)$, κ, and learning rates Γ_w and Γ_v, $\dot{L} \le 0$ everywhere outside a compact set that is entirely within the largest level set of L that itself lies entirely within D (Ref. 35). Throwing out the trivial $\|\boldsymbol{e}\| = 0$ case where $\dot{L} \le 0$ by Eq. (A10), then $\dot{L} \le 0$ when

$$\|\tilde{Z}\|_F \ge Z_m = \frac{a_1 + \sqrt{a_1^2 + 4a_0(\kappa - \|PB\|c_3)}}{\kappa - \|PB\|c_3}$$

or

$$\|\boldsymbol{e}\| \ge \frac{a_0 + a_1 Z_m}{\frac{1}{2}\lambda_{\min}(Q)} \tag{A12}$$

giving an upper bound on the size of the compact set, and so increasing $\lambda_{\min}(Q)$ and κ can be used to decrease the size of this compact set. Increasing learning rates will expand the level set in the direction of NN weight errors as seen in Eq. (A6) and vice versa, resulting in an upper and lower bound for learning rates for a given network size n_2, $\lambda_{\min}(Q)$, and κ. Therefore, for initial conditions within D, error e and $\tilde{Z}$ are uniformly ultimately bounded,[39] with the ultimate bound on reference model tracking error given by Eq. (A12) treated as an equality.

Acknowledgments

NASA Marshall Space Flight Center (MSFC) supported this research (Grant NAG 3-1638). Rolf Rysdyk of the University of Washington and Kerry Funston, Charles Hall, and John Hanson of NASA MSFC also provided important assistance.

References

[1] Hanson, J., "Advanced Guidance and Control Project for Reusable Launch Vehicles," AIAA Paper 2000-3957, Aug. 2000.

[2] Shtessel, Y., Hall, C., and Jackson, M., "Reusable Launch Vehicle Control in Multiple Time Scale Sliding Modes," *Journal of Guidance, Control, and Dynamics*, Vol. 23, No. 6, 2000, pp. 1013–1020.

[3] Shtessel, Y., Buffington, J., and Banda, S., "Multiple Timescale Flight Control Using Reconfigurable Sliding Modes," *Journal of Guidance, Control, and Dynamics*, Vol. 22, No. 6, 1999, pp. 873–883.

[4] Calise, A., and Rysdyk, R., "Nonlinear Adaptive Flight Control Using Neural Networks," *Control Systems Magazine*, Vol. 18, No. 6, 1998, pp. 14–25.

[5] Lewis, F., "Nonlinear Network Structures for Feedback Control," *Asian Journal of Control*, Vol. 1, No. 4, 1999, pp. 205–228.

[6] Brinker, J., and Wise, K., "Flight Testing of a Reconfigurable Flight Control Law on the X-36 Tailless Fighter Aircraft," *Journal of Guidance, Control, and Dynamics*, Vol. 24, No. 5, 2001, pp. 903–909.

[7] Calise, A., Lee, S., and Sharma, M., "Development of a Reconfigurable Flight Control Law for Tailless Aircraft," *Journal of Guidance, Control, and Dynamics*, Vol. 24, No. 5, 2001, pp. 896–902.

[8]Calise, A., Sharma, M., and Corban, J., "Adaptive Autopilot Design for Guided Munitions," *Journal of Guidance, Control, and Dynamics*, Vol. 23, No. 5, 2000, pp. 837–843.

[9]Idan, M., Johnson, M., and Calise., A., "Hierarchical Approach to Adaptive Control for Improved Flight Safety," *Journal of Guidance, Control, and Dynamics*, Vol. 25, No. 6, 2003, pp. 1012–1020.

[10]Kim, N., Calise, A., Hovakimyan, N., Prasad, J., and Corban, J., "Adaptive Output Feedback for High-Bandwidth Flight Control," *Journal of Guidance, Control, and Dynamics*, Vol. 25, No. 6, 2002, pp. 993–1002.

[11]Doman, D., and Ngo, A., "Dynamic Inversion-Based Adaptive/Reconfigurable Control of the X-33 on Ascent," *Journal of Guidance, Control, and Dynamics*, Vol. 25, No. 2, 2002, pp. 276–284.

[12]Wohletz, J., Paduano, J., and Maine, T., "Retrofit Reconfiguration System for a Commercial Transport," AIAA Paper 2000-4041, Aug. 2000.

[13]Bernstein, D., and Michel, A., "A Chronological Bibliography on Saturating Actuators," *International Journal of Robust and Nonlinear Control*, Vol. 5, No. 4, 1995, pp. 375–380.

[14]Saberi, A., Lin, Z., and Teel, A., "Control of Linear Systems with Saturating Actuators," *IEEE Transactions on Automatic Control*, Vol. 41, No. 3, 1996, pp. 368–378.

[15]Kothare, M., Campo, P., Morari, M., Nett, C., "A Unified Framework for the Study of Anti-windup Designs," *Automatica*, Vol. 30, No. 12, 1994, pp. 1869–1883.

[16]Hu, T., Lin, Z., and Chen, B., "An Analysis and Design Method for Linear Systems Subject to Actuator Saturation and Disturbance," *Proceedings of the American Control Conference*, IEEE Publ., Piscataway, NJ, 2000, pp. 725–729.

[17]Barbu, C., Reginatto, R., Teel, A., and Zaccarian, L., "Anti-windup Design for Manual Flight Control," *Proceedings of the American Control Conference*, IEEE Publ., Piscataway, NJ, 1999, pp. 3186–3190.

[18]Lu, P., "Tracking Control of Nonlinear Systems with Bounded Controls and Control Rates," *Automatica*, Vol. 33, No. 6, 1997, pp. 1199–1202.

[19]McHenry, R., Brand, T., Long, A., Cockrell, B., and Thibodeu, J., III, "Space Shuttle Ascent Guidance, Navigation, and Control," *Journal of the Astronautical Sciences*, Vol. 27, No. 1, 1979, pp. 1–38.

[20]Stoorvogel, A., and Saberi, A., "Output Regulation of Linear Plants with Actuators Subject to Amplitude and Rate Constraints," *International Journal of Robust and Nonlinear Control*, Vol. 9, No. 10, 1999, pp. 631–657.

[21]Wang, H., and Sun, J., "Modified Model Reference Adaptive Control with Saturated Inputs," *Proceedings of the 31st Conference on Decision and Control*, IEEE Publ., Piscataway, NJ, 1992, pp. 3255, 3256.

[22]Leonessa, A., Haddad, W., and Hayakawa, T., "Adaptive Control for Nonlinear Uncertain Systems with Actuator Amplitude and Rate Saturation Constraints," *Proceedings of the American Controls Conference*, IEEE Publ., Piscataway, NJ, 2001, pp. 1292–1297.

[23]Rovithakis, G., "Nonlinear Adaptive Control in the Presence of Unmodelled Dynamics Using Neural Networks," *Proceedings of the 38th IEEE Conference on Decision and Control*, IEEE Publ., Piscataway, NJ, 1999, pp. 2150–2155.

[24]Monopoli, R., "Adaptive Control for Systems with Hard Saturation," *Proceedings of the IEEE Conference on Decision and Control*, IEEE Publ., Piscataway, NJ, 1975, pp. 841–843.

[25]Ohkawa, F., and Yonezawa, Y., "A Discrete Model Reference Adaptive Control System for a Plant with Input Amplitude Constraints," *International Journal of Control*, Vol. 36. No. 5, 1982, pp. 747–753.

[26]Karason, S., and Annaswamy A., "Adaptive Control in the Presence of Input Constraints," *IEEE Transactions on Automatic Control*, Vol. 39, No. 11, 1994, pp. 2325–2330.

[27]Annaswamy, A., and Wong, J., "Adaptive Control in the Presence of a Saturation Non-Linearity," *International Journal of Adaptive Control and Signal Processing*, Vol. 11, No. 1, 1997, pp. 3–19.

[28]Hanus, R., Kinnaert, M, and Henrotte J.-L., "Conditioning Technique, a General Anti-windup and Bumpless Transfer Method," *Automatica*, Vol. 23, No. 6, 1987, pp. 729–739.

[29]McFarland, M., and Calise, A., "Multilayer Neural Networks and Adaptive Nonlinear Control of Agile Anti-Air Missiles," AIAA Paper 97-3540, Aug. 1997.

[30]Kim, B., and Calise, A., "Nonlinear Flight Control Using Neural Networks," *Journal of Guidance, Control, and Dynamics*, Vol. 20, No. 1, 1997, pp. 26–33.

[31]Hall, C., Gallaher, M., and Hendrix, N., "X-33 Attitude Control System Design for Ascent, Transition, and Entry Flight Regimes," AIAA Paper 98-4411, Aug. 1998.

[32]Yesildirek, A., and Lewis, F., "Feedback Linearization Using Neural Networks," *Automatica*, Vol. 31, No. 11, 1995, pp. 2539–2544.

[33]Kim, Y., and Lewis, F., *High-Level Feedback Control with Neural Networks*, World Scientific, Singapore, 1998, p. 47.

[34]Lewis, F., Yesildirek, A., and Liu, K., "Multilayer Neural-Net Robot Controller with Guaranteed Tracking Performance," *IEEE Transactions Neural Networks*, Vol. 7, No. 2, 1996, pp. 1–12.

[35]Johnson, E. N., "Limited Authority Adaptive Flight Control," Ph.D. Dissertation, School of Aerospace Engineering, Georgia Inst. of Technology, Atlanta, Dec. 2000.

[36]Calise, A., Hovakimyan, N., and Idan, M., "Adaptive Output Feedback Control of Nonlinear Systems Using Neural Networks," *Automatica*, Vol. 37, No. 8, 2001, pp. 1201–1211.

[37]McCarter, J., "Maveric Users Guide," NASA/MSFC/TD54, June 1999.

[38]Hanson, J., Coughlin, D., Dukeman, G., Mulqueen, J., and McCarter, J., "Ascent, Transition, Entry, and Abort Guidance Algorithm Design for X-33 Vehicle," AIAA Paper 98-4409, Aug. 1998.

[39]Narendra, K. S., and Annaswamy, A. M., "A New Adaptive Law for Robust Adaptation Without Persistent Excitation," *IEEE Transactions on Automatic Control*, Vol. 32, No. 2, 1987, pp. 134–145.